Low-Frequency Dielectric Properties for Diagnosis of Aging in Polymeric Cables

ANTONIO MOTORI,[1,*] GIAN CARLO MONTANARI,[1] and STANISLAW GUBANSKI[2]

[1]Faculty of Engineering, University of Bologna, 40136 Bologna, Italy, and [2]Royal Institute of Technology, 100 44 Stockholm, Sweden

SYNOPSIS

The results of thermally stimulated discharging currents and isothermal direct currents measurements, performed on crosslinked polyethylene cable models aged under different thermal and electrothermal stresses, are presented and discussed. It is shown that aging affects the low-frequency behavior of the polymer. The changes observed in the relaxation processes are related to those of other properties, e.g., density, melting enthalpy, electric strength, electrical conductivity, and microstructure, as well as to the degradation phenomena caused in the insulation by the applied stresses. The proposed techniques, therefore, prove to be an effective diagnostic tool for investigating the aging of polymeric insulating materials. © 1996 John Wiley & Sons, Inc.

INTRODUCTION

Polymers, such as ethylene-propylene rubber (EPR) and, mainly, crosslinked polyethylene (XLPE), are extensively used as insulating materials in high voltage cables.

Aging under service stresses involves chemical-physical and microstructural changes of the polymeric insulation, which can lead to a progressive loss of reliability and, finally, to the failure of the cable. As the life of the cable is related to the state of the insulation, identifying diagnostic techniques capable of assessing the level of degradation of the insulation is of fundamental importance.

The thermally stimulated discharging currents (TSDC) technique allows rapid characterization of the relaxation processes in insulating materials with high resolution,[1,2] and for this reason it is nowadays widely used.[3] This technique also proved to be suitable for the study of degradation processes, such as oxidation and water treeing, which take place in the polymeric insulation of a cable during aging.[4-8]

In this article, the low-frequency dielectric behavior of XLPE cable models, aged at different stresses and for various times, is investigated by the TSDC technique, as well as by measurement of isothermal direct currents (IDC). Both techniques can provide information on relaxations that occur in the frequency range 10^{-2} to 10^{-4} Hz. The effects of aging conditions on the relaxation processes and their characteristic parameters (intensity, frequency and temperature location, activation energy) are analyzed. Correlations with the chemical-physical and microstructural changes caused in the insulation by aging are finally made.

EXPERIMENTAL PROCEDURES

Material and Aging Procedures

The investigated XLPE cable models were manufactured from Union Carbide HFDE 4201 compound by a steam-curing process.[9] The final cable consisted of a copper wire conductor (1.8 mm diameter), a semiconducting layer (ethylene-vinylacetate copolymer filled with carbon black, 0.5 mm thick), and XLPE insulation (1.5 mm thick).

After a thermal pretreatment at 90°C for about 90 h, having the purpose to stabilize the material with respect to possible differences in manufacturing histories, samples of cable about 40 cm in length

* To whom correspondence should be addressed.

Journal of Applied Polymer Science, Vol. 59, 1715-1724 (1996)
 CCC 0021-8995/96/111715-10

Table I Aging Conditions and Property Values for the Cable Models Subjected to TSDC and IDC Measurements

Sp. #	Aging Stresses and Times	d/d_0 (25°C)	$\Delta H/\Delta H_0$	γ/γ_0 (80°C)	ES/ES_0 (25°C)
1	90°C–90 h	1	1	1	1
2	130°C–800 h	1.02	0.66	290	0.76
3	130°C –4863 h	1.05	0.12	417	0.67
4	110°C–8074 h	1.03	0.10	69	0.55
5	110°C–5633 h	1.02	0.41	2.1	0.80
6	12 kV–60°C–1133 h	1.02	1.24	7.2	0.83
7	12 kV–60°C–1367 h	1.02	1.22	1.3	0.90

The values of density, d, melting enthalpy, ΔH, electrical conductivity, γ, and electric strength, ES, are referred to those measured on the pretreated specimens (d_0, ΔH_0, γ_0, and ES_0); conductivity values were determined at 80°C and 2 h after voltage application.

were subjected to thermal, electrical, and electrothermal aging.

The thermal life tests were carried out in an oven over the temperature range 100 to 150°C.

The electrical and electrothermal life tests were performed in air at different levels of temperature (from 20 to 110°C) and voltage (from 4 to 70 kV).

The choice of the test temperatures derives from cable design and the need to achieve thermal degradation in a reasonable time. The maximum temperature that determines the ampacity in steady conditions is 90°C. However, higher temperatures are allowed in overload and/or short-circuit conditions (up to 150°C), even if for short times. As regards thermal endurance characterization, according to IEC 216 Standard,[10] the temperatures chosen for life tests must be high enough to allow relatively short test times, but not too high in order that the prevailing thermal aging mechanism does not change from the test temperatures to that used for thermal endurance characterization, i.e., the temperature index, TI, which corresponds to the time to end point of 20 000 h.[10] Accordingly, the lowest and highest test temperatures must provide times to end point, i.e., failure times, not shorter than ×5000 and 100 h, respectively, and extrapolation of the thermal endurance line to TI must not exceed 20°C.[10]

The electrical and electrothermal life tests were performed using the progressive censoring technique,[11] in which specimens are removed from aging after chosen times and subjected to diagnostic measurements. Both the life lines and the changes of significant properties (e.g., density, melting enthalpy, electric strenth, electrical conductivity, oxidation time, etc.) with aging time were, thus, singled out for the material.[9,11–13]

Some aged cable models, suitably selected on the basis of the results of the chemical-physical investigations, were subjected to TSDC and IDC measurements. The aging conditions, as well as the values of some of the most significant properties measured on these cable specimens, are summarized in Table I.

Measuring Techniques

The measurements of TSDC and IDC were performed according to the following procedures.

All TSDC measurements were carried out in helium on cable specimens about 10 mm in length over the temperature range −120 to 120°C, using the instrumentation described elsewhere.[14] Due to the cable thickness, a temperature gradient was present in the insulation during the test; however, it is reasonable to consider that it was the same for all the specimens investigated, thus affecting all the spectra in the same way. A two-terminal electrode configuration was used for the measurements, the HV and LV electrodes being the conductor wire, and a silver paint layer on the external insulation, respectively. Measurements performed by both evaporated gold electrodes and silver paint electrodes provided comparable results; thus, the second solution was adopted for all the TSDC measurements here reported. Initially, a cleaning run was performed on each specimen, in order to avoid possible effects of built-in stresses and charges on the TSDC spectra. Heating rates from 0.5 to 9°C/min were applied; the poling voltage, temperature, and time were 350 V, 110°C, and 10 min, respectively. Note that the poling voltage was kept intentionally low to avoid problems with charge injection and PD activity (poling voltage

and temperature must not be confused with aging voltage and temperature).

The analysis of the TSDC spectra obtained at different heating rates allowed to derive relaxation parameters,[1,2] such as the apparent activation energy, E, the equivalent frequency, f_m, and the current density, J_m, of the maximum; the charge released, Q (which is independent of the heating rate), was also calculated. The values of E for the different relaxation processes were calculated from the slope of the regression lines obtained by plotting $\ln(T_m^2/r)$ vs. $1/T_m$, according to the relationship:

$$T_m = [(Er\tau_o/k) \exp(E/kT_m)]^{1/2}$$

where r is the heating rate, τ_o is the relaxation time at infinite temperature (τ_o^{-1} is the frequency factor), k is the Boltzmann constant, and T_m is the temperature of the maximum of the relaxation peak.

The values of f_m for each relaxation process were derived from the equation:

$$f_m = (1/2\pi)\ (Er/kT_m^2)$$

The charge released, Q, was calculated by integrating the area under each TSDC peak, according to the equation:

$$Q = \int_{t1}^{t2} Idt = \int_{T1}^{T2} I(dt/dT)dT$$

where $dt/dT = 1/r$, while T_1 and T_2 are the temperatures that bound the peak.

The relaxation map analysis (RMA) was also performed on the same cable specimens by the fractional polarization technique,[15,16] which allows separation of the elementary peaks of a relaxation process and calculation of the relaxation times distribution and their activation enthalpies and entropies. The instrumentation, poling voltage, and time for RMA were the same as for TSDC experiments, while the poling temperature was varied from −60 to 110°C every 10°C and the temperature window was set at 10°C.

Regarding the IDC technique, charging currents (therefrom conductivity) were measured as a function of time, temperature, and electrical field, by the voltmeter-ammeter method, according to ASTM Standard D 257, with the cell and instrumentation described elsewhere.[12] A three-terminal electrode configuration was used for the measurements: the conductor wire was the HV electrode, while the LV and guard electrodes were obtained by gold coating the external surface of the insulation under vacuum. Measurements were performed in air from 55 to 90°C on specimens of cable about 40 mm in length. Constant voltages up to 3 kV (corresponding to maximum electrical fields up to 3 kV/mm) were applied. After charging, discharging currents were measured as a function of time by shorting the electrodes, in order to detect possible dielectric relaxation effects in the ultralow-frequency range ($<10^{-2}$ Hz).[17-20]

The electrical measurements described above were supported by chemical-physical investigation, such as Fourier transform infrared (FT-IR) spectroscopy, differential scanning calorimetry (DSC), and oxidative stability measurements; microstructural observations were also made by scanning electron microscopy (SEM) supported by x-ray microanalysis.[9,13]

EXPERIMENTAL RESULTS

TSDC Measurements

The TSDC spectra obtained for the specimens of Table I with a heating rate of 7°C/min are reported in Figures 1–5.

Tables II and III summarize the values of the relaxation parameters E, Q, I_m, f_m, and T_m for each cable model.

The values of f_m, obtained at the different heating rates for each relaxation, are reported in Figures 6 and 7, where f_m is plotted vs. $10^3/T$ (Fig. 7 also shows f_m values provided by IDC measurements, which will be discussed later).

The spectrum of the pretreated cable (Fig. 1) exhibits two relaxation modes. The former is very

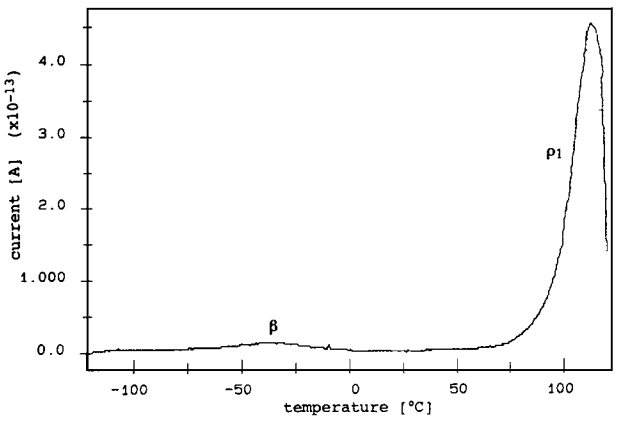

Figure 1 TSDC spectrum relevant to the pretreated cable specimen.

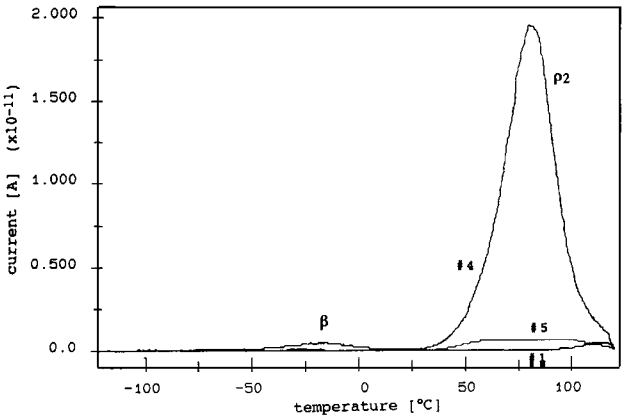

Figure 2 TSDC spectra relevant to cable specimens thermally aged at 110°C, compared with the pretreated one.

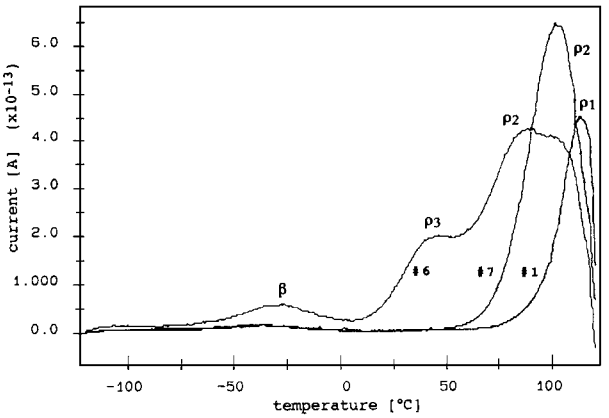

Figure 4 TSDC spectra relevant to cable specimens electrothermally aged at 12 kV–60°C, compared with the pretreated one.

weak, has its maximum at −39°C, and is characterized by an apparent activation energy of 98 kJ/mol. As discussed later, it has been associated with the β-relaxation.[21-25] The latter (hencefrom named ρ_1) exhibits the maximum at 108°C and can be related to the melting process of the crystalline fraction of XLPE. In fact, the maximum temperature of the peak is very close to the value of the melting temperature, 106°C, detected by DSC.[9] The apparent activation energy of the process is 135 kJ/mol.

Thermal aging at temperatures ≥ 110°C and electrothermal aging produce qualitative and quantitative changes in the TSDC spectra, as can be observed in Figures 1–7 and Tables II–III. On the contrary, negligible changes were observed in the spectra (as well as in the other properties investigated)[9,12] relevant to cables aged at temperatures < 110°C (even for longer times), which, therefore, will not be reported.

Regarding thermally aged cables, the remarkable changes in the parameters of the β-relaxation are pointed out in Figures 5–6 and Table II. As aging time increases, the β-relaxation becomes much stronger (Q and I_m increase) and its maximum shifts to higher temperatures, while its apparent activation energy rises. On the contrary, the intensity of the melting peak, ρ_1, decreases and its maximum shifts to slightly lower temperatures. The parameters relevant to this relaxation could be calculated only for the pretreated specimen. In fact, in the aged insulation it is hidden by a new peak, hencefrom named ρ_2, which appears at intermediate temperatures. Likewise the β-relaxation, also the ρ_2-peak (Figs. 2, 3, 7, and Table III) becomes stronger (Q and I_m increase) and its maximum shifts to higher temperatures with increasing aging time and stress. More-

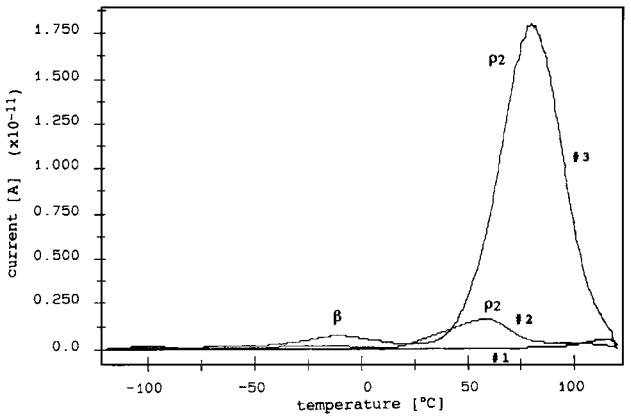

Figure 3 TSDC spectra relevant to cable specimens thermally aged at 130°C, compared with the pretreated one.

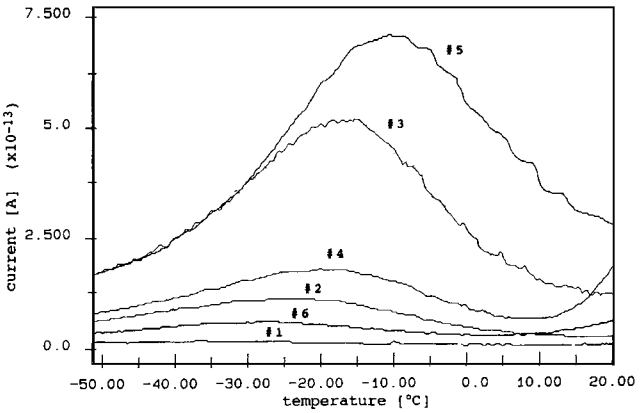

Figure 5 β-Relaxation for the cable specimens of Table I.

Table II Characteristic Parameters for the β-Relaxation

Sp. #	E (kJ/mol)	Q (C)	I_m (A)	f_m (Hz)	T_m (°C)
1	98	4.0×10^{-10}	1.5×10^{-14}	2.8×10^{-3}	−39
2	130	4.9×10^{-9}	1.8×10^{-13}	3.2×10^{-3}	−20
3	177	2.6×10^{-8}	7.2×10^{-13}	4.1×10^{-3}	−10
4	114	1.9×10^{-8}	5.4×10^{-13}	2.8×10^{-3}	−17
5	123	3.7×10^{-9}	1.1×10^{-13}	3.2×10^{-3}	−25
6	113	1.2×10^{-9}	6.0×10^{-14}	3.0×10^{-3}	−28
7	113	6.1×10^{-10}	1.9×10^{-14}	3.2×10^{-3}	−37

I_m, f_m, and T_m are relevant to a heating rate of 7°C/min.

over, the temperature of the maximum is higher for the specimens with lower melting enthalpy, i.e., lower crystallinity.

Similar, but much smaller, changes in the activation energy, intensity, charge released, and temperature location of the β-relaxation are exhibited by the electrothermally aged cables, depending on aging stress and time (Figs. 4–6 and Table II). Negligible changes were observed for the ρ_1-peak (being partly or fully hidden by the intermediate peak, its parameter values can hardly be calculated). The intermediate relaxation, ρ_2, is slightly separated from the melting one in the cable aged at 12 kV–60°C for 1133 h, while in that aged for 1367 h it fully hides the melting peak. However, the intensity of this relaxation is considerably lower than that previously exhibited by thermally aged cables. Moreover, a fourth peak, hencefrom named ρ_3, is present around 40°C only at the former aging time (Fig. 4).

IDC Measurements

The dielectric loss factor, ε'', in the ultralow-frequency region was obtained from isothermal discharging currents, according to the well-known Hamon relationship:[17]

$$\varepsilon'' = J/(2\pi f \varepsilon_o F)$$

where J is the current density, $f = 0.1/t$ is the equivalent frequency, ε_o is the permittivity of vacuum, and F is the electrical field.

A thermally activated relaxation process was pointed out in the aged cables, as shown, for example, in Figures 8 and 9, where ε'' is plotted vs. frequency at various temperatures for specimens #2 and #6, respectively. As can be observed, the relaxation is much stronger in the thermally aged specimens than in the electrothermally aged ones. On the contrary, relaxation peaks were not detected in the pretreated specimen.

The frequency of the maximum of these loss factor peaks is plotted vs. $1000/T$ in Figure 7 and compared with the corresponding values relevant to the intermediate peak, ρ_2, provided by TSDC measurements at different heating rates.

Conductivity, derived from charging currents at 2 h after voltage application, is plotted vs. the reciprocal absolute temperature in Figure 10. While the thermally aged cables exhibit a strong increase with aging time and stress (see also Table I), the samples electrothermally aged at 12 kV–60°C show a notmonotone behavior, as can better be observed in Figure 11: conductivity increases with aging time up to a maximum after about 1133 h, then it decreases to values slightly higher than the initial one. The values of the apparent activation energy, E, for

Table III Characteristic Parameters for the ρ_2-Relaxation (I_m, f_m, and T_m are Relevant to a Heating Rate of 7°C/min.

Sp. #	E (kJ/mol)	Q (C)	I_m (A)	f_m (Hz)	T_m (°C)
2	101	5.9×10^{-8}	1.6×10^{-12}	1.5×10^{-3}	58
3	114	4.8×10^{-7}	1.8×10^{-11}	1.5×10^{-3}	81
4	116	1.9×10^{-8}	2.0×10^{-11}	1.5×10^{-3}	82
5	138	—	7.0×10^{-13}	1.9×10^{-3}	69

I_m, f_m, and T_m are relevant to a heating rate of 7°C/min.

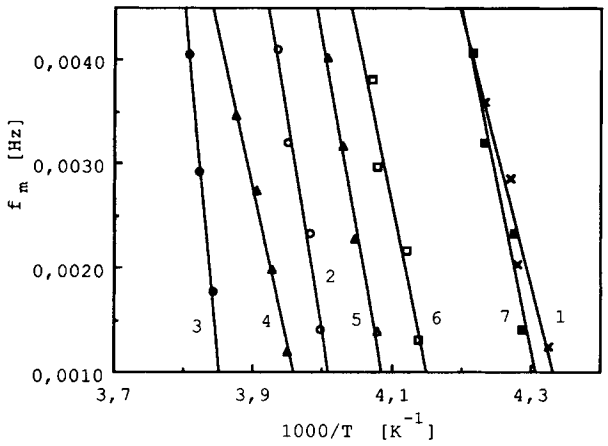

Figure 6 Temperature location of the maximum frequency, f_m for the β-relaxation.

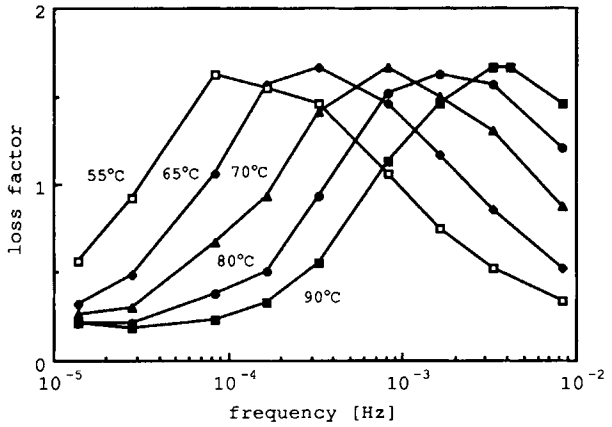

Figure 8 Relaxation process pointed out by IDC measurements in specimen #2.

both the relaxation process and conductivity, derived from the slope of the IDC regression lines of Figures 7 and 10, respectively, are compared in Table IV with those relevant to the intermediate relaxation process, ρ_2, detected by TSDC. For each cable specimen, the values of E for the three processes are quite close, considering that two different methods were used (each of them affected by its own measurement and data-processing errors). This leads to argue that both TSDC and IDC point out the same process and that it has the same origin as the conduction process.

DISCUSSION

The observed relaxation processes and their variations with aging can be related to the chemical-physical and microstructural changes caused in the insulation by the applied stresses.

Termally Aged Cables

As summarized in Table I, remarkable increase of density and conductivity and decrease of melting enthalpy (i.e., crystallinity) and electric strength were observed in the cables aged at temperatures $\geq$ 110°C, i.e., higher than the melting point (106°C) of the crystalline regions of the insulation. With increasing aging time and stress, FT–IR absorption spectroscopy revealed an intensity increase of the peaks over the range 1720–1740 cm^{-1}, thus indicating an increase of the concentration of the carbonyl groups. Moreover, enlargement of the distributed microcracks, which were already present in the pretreated cables, was observed.[9] These results allowed

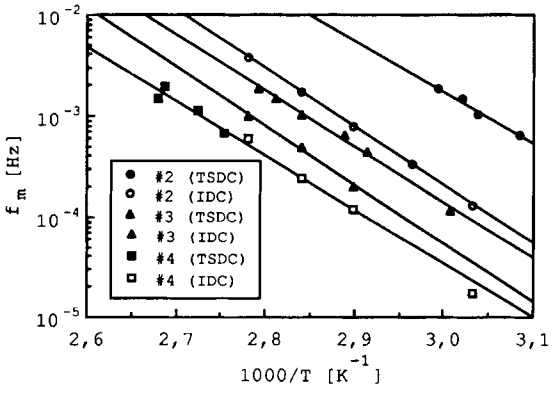

Figure 7 Temperature location of the maximum frequency, f_m, for the ρ_2-relaxation in TSDC spectra and the relaxation process singled out by IDC measurements.

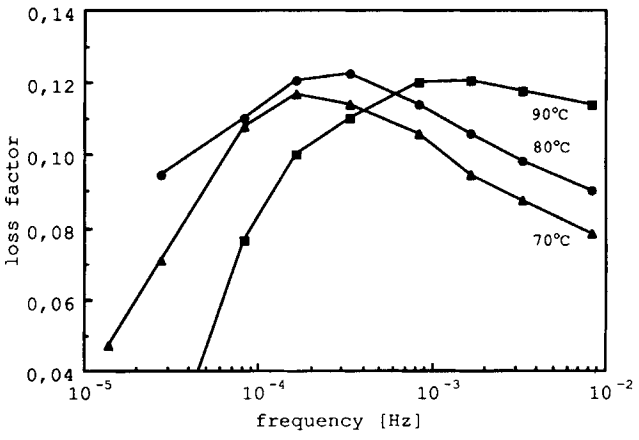

Figure 9 Relaxation process pointed out by IDC measurements in specimen #6.

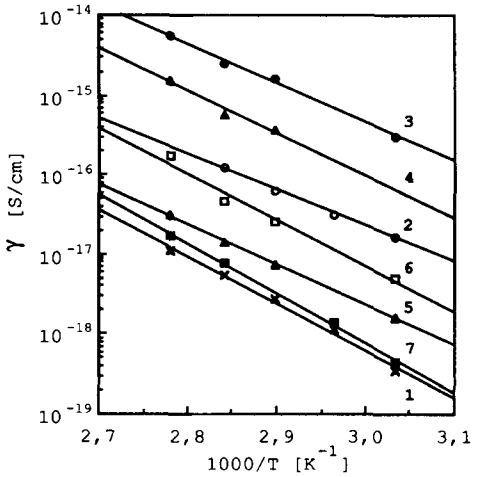

Figure 10 Conductivity, γ, vs. reciprocal absolute temperature for the cable specimens of Table I.

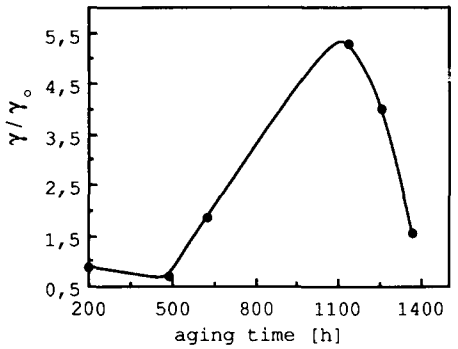

Figure 11 Conductivity, γ, vs. aging time for cable specimens aged at 12kV–60°C (values are referred to that of the pretreated specimen, γ_o).

to ascertain that bulk thermo-oxidative processes play a prominent role in the aging of the cables at these temperatures. Mainly crystalline regions, which are practically antioxidant free and are melted during aging, undergo strong oxidative degradation; degradation phenomena, such as chain scission and crosslinking, take place. The processes summarized in this picture are responsible for the observed property changes. On the contrary, only slight variations of the same properties were detected for aging at temperatures < 110°C,[9,12] even after long times (up to 20,000 h), thus indicating that oxidation takes place at significantly lower rate and concerns mostly the amorphous fraction of the insulation.

The TSDC and IDC results confirm this picture. In fact, aging at temperatures ≥ 110°C strongly affects the electrical behavior of the cables, causing qualitative and quantitative changes in the relaxation spectrum, as well as increase of conductivity; lower thermal stresses do not significantly affect the electrical properties.

The low-temperature TSDC peak can be identified as the β-relaxation and related to the glass–rubber transition of the amorphous region of the polymer[21–26] (even if controversial interpretations on the nature of this relaxation in polyethylene are given in literature).[27] This interpretation is supported by the fact that the temperature location of the peak is close to the glass-transition temperature, T_g, measured by DSC. Shifting of the relaxation maximum to higher temperatures with thermal aging can be related to the chemical-physical changes observed in the material. In particular, decrease of melting enthalpy and increase of density mean increase of the amorphous fraction and crosslinking due to oxidation. As a consequence, T_g increases and the maximum of the relaxation process shifts. Moreover, as the β-relaxation is ascribed to the polar groups attached to the polymer chains in the amorphous region,[24] the higher values of intensity, I_m, and charge released, Q, observed for this process in the aged cables can be associated to the higher carbonyl groups concentration detected by FT–IR spectroscopy. In fact, a direct relation between the concentration of the carbonyl groups spectroscopically determined and the charge released was pointed out elsewhere.[22,23] Referring to the apparent activation energy of the process, the higher values derived for the heavily aged cables (e.g., E = 177 kJ/mol for specimen #3 in Table II) are not far from that (E = 212 kJ/mol) obtained by other authors from dielectric measurements on oxidized low-density polyethylene.[24]

The relaxation mode characteristic of the aged cables, ρ_2, which ranges from about 60 to 80°C (depending on the aging conditions), and the thermally

Table IV Comparison between the Apparent Activation Energies of ρ_2 Relaxation in TSDC Spectra ($E_{\rho 2}$), Ultralow Frequency Relaxation from Isothermal Depolarization Currents (E_{dep}) and Isothermal Conductivity (E_γ)

Sp. #	$E_{\rho 2}$ (kJ/mol)	E_{dep} (kJ/mol)	E_γ (kJ/mol)
2	101	110	101
3	114	122	100
4	116	116	112
5	138	133	105
6	n.d.	149	132

activated peak disclosed by data treatment of isothermal discharging currents at close temperatures and frequencies should arise from the same polarization process. Even the values of the apparent activation energy, E, obtained by the two techniques are in good agreement. The different methods used and their approximations can explain shiftings sometimes observed in the frequency/temperature location and activation energy. Moreover, as this relaxation is characterized by values of E quite close to those found for the conduction process, it should be ascribed to the same mechanism that rules conduction,[1,28] i.e., motion of charge carriers. The charge origin of the ρ_2-peak is also supported by the results obtained by other authors on different types of polyethylene[5,29,30] (however, a partial contribution of dipoles cannot be excluded).[5] Charge polarization takes place at the interfaces of the insulation, i.e., the insulation/semiconducting layer interface and the distributed microcracks present in the polymer matrix enlarging with aging. This is confirmed by the results of IDC measurements performed on the insulation after removing the semiconducting layer: the peak was still present, but its intensity was strongly reduced.

The high-temperature peak, ρ_1, detected in both the pretreated and aged cable models, can be related to the melting process of the crystalline regions of the polymer. In fact, as aging goes on, the intensity of the peak decreases and its maximum shifts to a slightly lower temperature, while, at the same time, even melting temperature and enthalpy decrease (Table I). For the pretreated cable, the values of E relevant to both this relaxation mode and conduction are almost coincident, i.e., 135 and 144 kJ/mol for the former and the latter, respectively (these values could not be calculated for the aged cables, due to peak overlapping). Therefore, even this process can be ascribed to charge polarization at the interfaces between crystalline and surrounding amorphous regions. Its intensity decrease with aging can be related to a reduction of these interfaces as a consequence of crystallinity decrease.

A further support to the above-discussed charge or molecular nature of the detected peaks is provided by RMA results: a "normal" distribution of elementary peaks, which is characteristic of molecular relaxations,[30] was exhibited only by the β-peak; on the contrary, the intermediate and, mainly, the high-temperature peak did not show a "normal" property, thus indicating for a charge polarization process.[7,8]

Regarding the nature of the charge carriers in XLPE, the analysis of charging and discharging currents vs. time and temperature,[12] as well as the consideration that thermo-oxidative processes taking place during thermal aging, can enhance ionic conduction and AC losses at low frequency,[31,32] led to hypothesize that ions should be the major carriers in the ranges of temperature and electrical field investigated.[12] Actually, oxidation products can act as localized centers (associated with the carbonyl groups) by which hopping of injected electrons occurs.[33] However, the fact that reversals and/or other anomalous behaviors were not observed both in isothermal currents and in TSDC spectra seems to allow to rule out electron injection (indeed, the values of applied electrical field are about one order of magnitude lower than the values that usually cause charge carriers injection and anomalous currents).[34,35] Finally, these assumptions are also supported by the results of IDC measurements on specimens of aged cables with different electrode materials (gold and carbon): no differences were observed in the behavior of charging/discharging currents vs. time, conductivity values, intensity, and temperature location of the ρ_2-relaxation.

Electrothermally Aged Cables

As shown in Table I, electrothermal aging caused variations of the investigated properties that are much lower than those detected for thermal aging at temperatures $\geq 110°C$, but anyhow higher than for aging at temperatures $< 110°C$ (even for longer times). This clearly revealed a synergistic effect of electrical field and temperature.[9] Moreover, a nonmonotone behavior of the properties with aging time was observed,[9,36] as shown, for example, in Figure 11 for conductivity. The synergistic action of multistress enhanced matter transport phenomena in the bulk of the insulation and led to formation of heterogeneous regions in which impurities, already present in the bulk of the insulation and/or in the semiconducting shield, concentrated.[9] These regions were observed to increase in number with aging time. Starting from a time dependent on the aging conditions (about 800 h for the cables aged at 12 kV–60°C), their morphology changed and microcracks formed and enlarged at the interface with the surrounding matrix. Multistress also caused a mild bulk oxidation, mainly localized in the amorphous region of the insulation, as evidenced by the small property changes detected.[9]

These findings can help to explain the isothermal and TSDC results previously reported.

Regarding the β-relaxation, the intermediate peak, ρ_2, and the melting peak, ρ_1, the small vari-

ations detected in the electrothermally aged samples can be explained with the lower chemical-physical changes caused in the insulation bulk by multistress, in comparison with thermal aging at high temperatures. In the case of electrothermal aging, in fact, insulation failure is a localized phenomenon, due to electric field concentration that overcomes the electric strength of the insulation. Therefore, failure generally occurs before the establishment of a significant bulk degradation. However, the considerations on the nature of the relaxation processes detected by TSDC and the correlations with other properties, previously made for thermal aging, hold also for multistress aging.

The different characteristics of TSDC spectra at intermediate temperatures can be related to the microstructural features and nonmonotone behavior of the properties pointed out for the electrothermally aged cables. In particular, the ρ_3-peak is present only in the cable aged at 12 kV–60°C for 1133 h, i.e., in correspondence of the maximum of conductivity curve vs. aging time (Fig. 11). For shorter and longer aging times this peak was not observed, while the conductivity values are lower, approaching that of the pretreated cable. The maximum in the conductivity vs. aging time curve and ρ_3-relaxation process can be related to the appearance and spreading of the heterogeneous regions previously described. Release of charge carriers and their migration to low-density regions could be related to the rising part of the curve of Figure 11 and to the appearance of the peak, while the subsequent decrease of conductivity could be associated to trapping of charge carriers by the heterogeneous regions in a further stage of aging, when they enlarge and microcraks start to form at the regions–matrix interfaces. At this stage of aging, only the ρ_2-relaxation process, which is ascribed to interfaces, is observed.

CONCLUSIONS

The TSDC spectra of the investigated XLPE cable models exhibit several relaxation modes. Only two modes are present in the pretreated specimen, i.e., the β-relaxation, related to the glass–rubber transition of the amorphous region, and a high-temperature peak, ascribed to charge polarization and related to the melting of the crystalline region of the polymer.

Aging produces variations of the characteristics of these relaxations, as well as the appearance of new peaks, which may likely be ascribed to charge polarization.

The changes observed in the relaxation processes with aging time and stress are related to those of other properties investigated (e.g., density, melting enthalpy and temperature, electric strength, and DC conductivity) and to the chemical-physical and microstructural changes caused in the insulation by aging.

The investigation performed proves that both TSDC and IDC techniques provide information for the diagnosis of aging in polymeric cable insulation.

REFERENCES

1. J. Van-Turnhout, *Thermally Stimulated Discharge of Polymer Electrets,* Elsevier, Amsterdam, 1975.
2. P. Braunlich, in *Topics in Applied Physics,* Vol. 37, Springer-Verlag, Berlin, 1979.
3. C. Lavergne and C. Lacabanne, *IEEE Electr. Insul. Magn.,* **9**(2), 5 (1993).
4. M. Ieda, T. Mizutani, Y. Suzuoki, and Y. Yokota, *IEEE Trans. Electr. Insul.,* **25**(3), 509 (1990).
5. A. Svatik, P. C. N. Scarpa, D. K. Das-Gupta, and D. E. Cooper, Proc. CEIDP Conf., Pocono Manor, PA, 1992, p. 475.
6. S. M. Gubanski, S. Bamji, and A. Bulinski, Proc. CEIDP Conf., Pocono Manor, PA, 1993, p. 732.
7. A. Motori, G. C. Montanari, and S. Gubanski, Proc. CEIDP Conf., Pocono Manor, PA, 1993, p. 751.
8. S.M. Gubanski, G. G. Montanari, and A. Motori, Conf. Rec. IEEE Int. Symp. on Electr. Insul., Pittsburgh, PA, 1994, p. 54.
9. A. Motori, F. Sandrolini, and G. C. Montanari, *IEEE Trans. Power Del.,* **6,** 34 (1991).
10. IEC 216 Standard, *Guide for Determination of Thermal Endurance Properties of Electrical Insulating Materials*, Fourth issue (1990–1994).
11. G. C. Montanari and M. Cacciari, *IEEE Trans. Electr. Insul.,* **23,** 365 (1988).
12. A. Motori, F. Sandrolini, G. C. Montanari, and M. Loggini, Conf. Rec. 3rd ICPADM, Tokyo, Japan, 1991, p. 761.
13. S. Bamji, A. Bulinski, J. Densley, G. C. Montanari, and A. Motori, Conf. Rec. IEEE Int. Symp. on Electr. Insul., Baltimore, MD, 1992, p. 44.
14. S. M. Gubanski, U. Nilsson, and M. S. E. Wang, Proc. NORD-IS 92 Conf., Vasteras, Sweden, 1992, p. 8.5.1.
15. M. Zielinski and M. Kryszewski, *Pys. Stat. Sol. (A),* **42,** 305 (1977).
16. J. Ibar, P. Barnes, P. Denning, T. Thomas, J. Saffel, P. Jones, A. Bernes, M. Rodrigues. and C. Lacabanne, *ANTEC '88,* 1049 (1988).
17. B. V. Hamon, *Proc. IEE,* **99**(part IV), 151 (1952).
18. M. E. Baird, *Prog. Polym. Sci.,* **1,** 161 (1967).
19. H. J. Wintle, *Solid-State Electron.,* **18,** 1039 (1975).

20. F. Sandrolini, A. Motori, and A. Saccani, *J. Appl. Polym. Sci.*, **44,** 765 (1992).
21. J. Hoffman, G. Williams, and E. Passaglia, *J. Polym. Sci. C,* **14,** 173 (1966).
22. P. Fisher and P. Rohl, *J. Polym. Sci., Polym. Phys. Ed.,* **14,** 531 (1976).
23. P. Fisher and P. Rohl, *Ibid,* 543 (1976).
24. C. Ashcraft and R. Boyd, *J. Polym. Sci., Polym. Phys. Ed.,* **14,** 2153 (1976).
25. R. H. Boyd, *Polymer,* **26,** 323 (1985).
26. Y. P. Khanna, E. A. Turi, T. Taylor, V. V. Vickroy, and R. F. Abbott, *Macromolecules,* **18,** 1302 (1985).
27. R. Popli, M. Glotin, and L. Mandelkern, *J. Polym. Sci., Polym. Phys. Ed.,* **22,** 407 (1974).
28. J. Vanderschueren and J. Gasiot, in *Topics in Applied Physics,* Vol. 37, Springer-Verlag, Berlin, 1979.
29. P. Colomer Vilanova, S. Montserrat-Ribas, M. A. Ribes-Greus, J. M. Meseguer-Duenas, J. L. Gomez-Ribelles, and R. Diaz-Calleja, *Polym.-Plast. Technol. Eng.,* **37**(7&8), 635 (1989).
30. S. M. Gubanski, K. Karlsson, and U. Gedde, Conf. Rec. IEEE Int. Symp. on Electr. Insul., Baltimore, MD, 1992, p. 161.
31. M. E. Baird, *Electrical Properties of Polymeric Materials,* The Plastic Inst., London, 1973.
32. J.-P. Crine, S. Pelissou, Y. McNicoll, and H. St-Onge, Conf. Rec. 2nd ICPADM, Beijng, China, 1988, p. 9.
33. T. Mizutani, T. Tsukahara, and M. Ieda, *J. Phys. D: Appl. Phys.,* **13,** 1673 (1980).
34. T. Hashimoto, M. Shiraki, and T. Sakai, *J. Polym. Sci., Polym. Phys. Ed.,* **13,** 2401 (1975).
35. H. J. Wintle, *IEEE Trans. Electr. Insul.,* **EI-21,** 747 (1986).
36. A. Motori, F. Sandrolini, and G. C. Montanari, Proc. IEEE Int. Conf. on Conduction and Breakdown in Solid Dielectrics, Sestri Levante, Italy, 1992, p. 285.

Received March 20, 1995
Accepted October 9, 1995